Asia Pacific Journal of Mathematics, Vol. 5, No. 1 (2018), 109-131 ISSN 2357-2205

DYNAMICAL BEHAVIORS OF TRAVELING WAVE SOLUTIONS OF A GENERALIZED K(N, 2N, -N) EQUATIONS

TEMESGEN DESTA LETA[1] & JIBIN LI[1,2,*]

[1]Department of Mathematics, Zhejiang Normal University, Jinhua, 321004, Zhejiang, P.R.China
[2]School of Mathematical Sciences, Huaqiao University, Quanzhou, 362021, Fujian, P. R. China
[*]Corresponding author: lijb@zjnu.cn

Received Jan 1, 2018

Abstract. In this paper, the analytical and numerical evaluation of a generalized K(n, 2n, -n) equation is studied by the qualitative theory of bifurcations method. The result shows the existence of the different kinds of traveling wave solutions of the generalized K(n, 2n, -n) equation, including solitary waves, kink and anti-kink waves, periodic wave and compacton wave, which depend on different parametric ranges. These results completely improve the study of traveling wave solutions for the mentioned model stated in Wazwaz (App. Math. & Compu. **173** (2006) 213-230).

2010 Mathematics Subject Classification. 34A05, 34C25-28, 34M55.
Key words and phrases. solitary wave solution; periodic wave solution; kink and anti-kink wave solution; compacton wave solution; exact solution; dynamical behavior.

1. Introduction

The study of traveling wave solutions in particular, solitons, of partial deferential equations (PDEs), for various nonlinear evolution equations in mathematical physics plays an important role. To obtain the traveling wave solutions for PDEs, a lot of systematic methods have been developed, such as the inverse scattering method, the Bácklund and the Darboux transformations, the tanh-function method, the homogeneous balance method, the extended tanh-function method and others [1, 2, 3, 4].

It is well known that solitons appear as a result of a balance between the nonlinear convection uu_x and the linear dispersion u_{xxx} in the integrable nonlinear KdV equation

$$u_t + auu_x + bu_{xxx} = 0; \tag{1}$$

gives rise to solitons: waves with infinite support. Unlike the standard KdV soliton which narrows as the amplitude increases [5], the compactons width is independent of the amplitude. In other words, the compacton is a soliton characterized by the absence of infinite wings or tails. The soliton concept appeared for the first time in the context of nonlinear lattices, then became a reality in many branches of science.

In nonlinear fiber optics, the long range interaction of solitons imposes a strict limitation on the performance of long-haul fiber transformation [6]. The famous article of Rosenau and Hyman was one of the first to call broad attention to the compactons phenomenon. The concept of compactons: solitons with compact support, or strict localization of solitary waves, appeared in [7, 8] where a genuinely nonlinear dispersive equation K(n,n) a special type of the KdV equation defined by

$$u_t + a(u^n)_x + (u^n)_{xxx} = 0, \quad n > 1, \tag{2}$$

that is a delicate interaction between a nonlinear convection $(u^n)_x$ with the genuine nonlinear dispersion $(u^n)_{xxx}$ that generates solitary waves with exact compact support.

In this paper we consider the generalized K(n, 2n, -n) equation,

$$u_t + a(u^n)_x + \left[bu^{2n}(u^{-n})_{xx}\right]_x = 0, \quad n > 1, \tag{3}$$

where a and b are two non-zero real number. Recently, by using the sine-cosine method and the tanh method, Wazwaz [9] found for $\frac{a}{b} > 0$ a family of compact solutions:

$$u_1(x,t) = \begin{cases} \{\frac{2nc}{a(3n-1)} \sin^2\left(\frac{n-1}{2n}\sqrt{\frac{a}{b}}(x-ct)\right)\}^{\frac{1}{n-1}}, & |\mu\xi| < \pi, \\ 0, & \text{otherwise} \end{cases}$$

$$u_1(x,t) = \begin{cases} \{\frac{2nc}{a(3n-1)} \cos^2\left(\frac{n-1}{2n}\sqrt{\frac{a}{b}}(x-ct)\right)\}^{\frac{1}{n-1}}, & |\mu\xi| < \frac{\pi}{2}, \\ 0, & \text{otherwise} \end{cases}$$

for other exact explicit solutions the reader may see [10]. However, the bifurcation behavior of the traveling wave solutions for corresponding traveling wave equations haven't studied in its parameter space. It is very important to understand the dynamical behavior of solutions for the traveling wave equation (3) in its parameter space.

To study the traveling wave solutions of equation (3), we substitute

$$u(x,t) = u(\xi) = \phi(\xi), \quad \xi = x - ct, \tag{4}$$

with wave speed c. Substituting equation (4) in to equation (3) and integrating once we obtain the following auxiliary ordinary differential equation:

$$bn\phi^{n-1}\phi_{\xi\xi} - bn(n+1)\phi^{n-2}\phi_\xi^2 - a\phi^n + c\phi - c_1 = 0, \tag{5}$$

where, c_1 is an integral constant, equation (4) is equivalent to the planner dynamical system:

$$\frac{d\phi}{d\xi} = y, \quad \frac{dy}{d\xi} = \frac{n(n+1)\phi^{n-2}y^2 + \alpha(\phi^n - \beta\phi + \gamma)}{n\phi^{n-1}}, \tag{6}$$

which has the first integral

$$H(\phi, y) = \frac{1}{2\phi^{2(n+1)}}y^2 + \frac{\alpha}{\phi^{3n}}\left(\frac{1}{2n}\phi^n + \frac{\beta}{1-3n}\phi + \frac{\gamma}{3n}\right) = -h. \tag{7}$$

where, $\alpha = \frac{a}{b}$, $\beta = \frac{c}{a}$ and $\gamma = \frac{c_1}{a}$.

Clearly, system (6) is a singular traveling wave system of the first class defined by [11, 12] with one singular straight line $\phi = 0$. Because the phase orbits defined by the vector fields of system (6) determine types of traveling wave solutions of equation (3), we are going to find all period annuluses and their boundary curves for system (6) and to describe all bifurcations of phase portraits on the (ϕ, y)-phase plane and the bifurcation set on the parameter space $(\alpha,\ \beta,\ \gamma)$ for system (6). We focus on the bounded traveling wave solutions and we give all possible exact explicit parametric representations for the traveling wave solutions of system (6).

This paper is organized as follows. In Sect. 2, we study the dynamical behavior of system (6) when $n = 2m$ and $n = 2m + 1,\ m \geq 1$ in the (ϕ, y) - plane. In Sects. 3 and 4, we investigate the exact solutions of equation (3) when $n = 2$ and $n = 3$ respectively.

2. Bifurcations of phase portraits of system (6)

In this section, we study all possible phase portraits defined by system (6) when the parameter $(\alpha,\ \beta,\ \gamma)$are varied. Let $d\xi = n\phi^{n-1}d\zeta$. Then except on the straight line $\phi = 0$, system (6) has the same topological phase portraits as the following associated regular system:

$$\frac{d\phi}{d\zeta} = ny\phi^{n-1}, \quad \frac{dy}{d\zeta} = n(n+1)\phi^{n-2}y^2 + \alpha(\phi^n - \beta\phi + \gamma). \tag{8}$$

The dynamics of system (8) and (6) are different in the neighborhood of the straight line $\phi = 0$. Specially, under some parameter conditions, the variable ζ is a fast variable while the variable ξ is a slow variable in the sense of the geometric singular perturbation theory.

For $n = 2$, $\alpha\gamma > 0$ and $\beta^2 - 4\gamma > 0$, system (6) has two equilibrium points $A_{1,2} = (\phi_{1,2}, 0)$, where $\phi_1 = \frac{\beta - \sqrt{\beta^2 - 4\gamma}}{2}$, $\phi_2 = \frac{\beta + \sqrt{\beta^2 - 4\gamma}}{2}$. On the straight line $\phi = 0$, there are two equilibrium points $Q_{1,2}(0, \pm\frac{1}{6}\sqrt{Y_s})$ with $Y_s = -6\alpha\gamma$, if $Y_s > 0$. Note that as $H(\phi_i, y_i) = h_i$ changes, system (6) defines different families of orbits of system (7) with different dynamical behavior. For the function defined by (7) we have $h_0 = H(0, 0)$,

$$h_1 = H(\phi_1, 0) = \alpha(\phi_1)^{-3n}\left(\frac{1}{2n}\phi_1^n + \frac{\beta}{1-3n}\phi_1 + \frac{\gamma}{3n}\right)$$

$$h_2 = H(\phi_2, 0) = \alpha(\phi_2)^{-3n}\left(\frac{1}{2n}\phi_2^n + \frac{\beta}{1-3n}\phi_2 + \frac{\gamma}{3n}\right)$$

Specially, for $\gamma = \frac{6}{5}\beta^2$, and $n = 2$ we have $H(\phi_1, 0) = H(0, \pm Y_s) = 0$.

Let $M(\phi_j, y_j)$ be the coefficient matrix of the linearized system of (8) at an equilibrium point $E_j(\phi_j, y_j)$ and $J(\phi_j, y_j)$ is the corresponding Jacobian determinant of the $M(\phi_j, y_j)$.

$$\begin{aligned} J(\phi_1, 0) &= \mathrm{detM}(\phi_j, 0) = -n\alpha\phi_1^{n-1}(n\phi_1^{n-1} - \beta), \\ J(\phi_2, 0) &= \mathrm{detM}(\phi_2, 0) = -n\alpha\phi_2^{n-1}(n\phi_2^{n-1} - \beta), \\ J(\phi_j, y_j) = \mathrm{detM}(\phi_j, y_j) &= n^2(n^2-1)\phi_i^{2(n-2)}y_i^2 - n\alpha\phi_i^{n-1}(n\phi_i^{n-1} - \beta). \end{aligned} \tag{9}$$

By the theory of planar dynamical systems [13, 14, 15], for an equilibrium point of a planar integrable system, (i) If $J < 0$, then the equilibrium point is a saddle point. (ii) If $J = 0$ and the Poincaré index of the equilibrium point is zero, then the equilibrium point is a cusp point. (iii) If $J > 0$ and trace(M) $= 0$, then the equilibrium point is a center point. (iv) if $J > 0$ and $(\mathrm{trace(M)})^2 - 4J > 0$, then the equilibrium point is a node point.

Corresponding to the phase curves we need to consider two different cases. For $n \geq 2$, the straight lines $\phi = 0$ is an integral invariant straight line of system (8). Denote that, $f(\phi) = \phi^n - \beta\phi + \gamma$. So, $f'(\phi) = n\phi^{n-1} - \beta$. Here we consider two sub-folds, for odd and even positive integers, we choose respectively $n = 2m+1$ and $n = 2m$. Let $\phi_0 = \left(\frac{\beta}{n}\right)^{\frac{1}{n-1}}$, for $n \neq 0$. Here $f'(\pm\phi_0) = 0$. We have $f_{\{n=2m\}}(\phi_0) = \gamma + \left(1 - n^{\frac{n}{n-1}}\right)\left(\frac{\beta}{n}\right)^{\frac{n}{n-1}}$ and $f_{\{n=2m+1\}}(-\phi_0) = \gamma - \left(1 - n^{\frac{n}{n-1}}\right)\left(\frac{\beta}{n}\right)^{\frac{n}{n-1}}$.

Thus, we have four level curves that partitioned the (β, γ)-parameter plane into subregions for $f_{\{2m\}}$ and $f_{\{2m+1\}}$ as shown in Fig. 1 (a) and Fig. 1 (b) respectively ;

$$\Pi_1 : \ \gamma = 0, \ \text{and} \ \Pi_2 : \gamma = -\left[\left(\frac{1}{2m}\right)^{\frac{2m}{2m-1}} - \left(\frac{1}{2m}\right)^{\frac{1}{2m-1}}\right]\beta^{\frac{2m}{2m-1}},$$

$$T_1 : \ \gamma = 0, \ \text{and} \ T_2 : \gamma = \left[1 - (2m+1)^{\frac{2m+1}{2m}}\right]\left(\frac{\beta}{2m+1}\right)^{\frac{2m+1}{2m}},$$

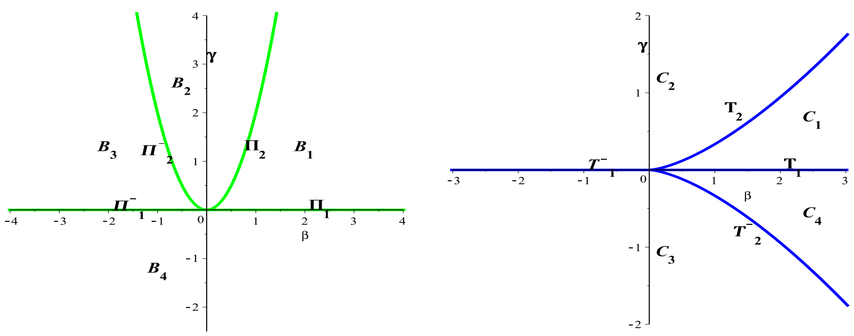

(a) $n = 2m$ (b) $n = 2m+1$

Figure 1. Regions partitioned by bifurcation curves in the (β, γ)-plane for $m \in \mathbb{Z}^+$

By using the above information to do qualitative analysis for $\alpha > 0$ and $\alpha < 0$, we have the following bifurcations of the phase portraits of system (6) shown in Fig.2 - Fig.5.

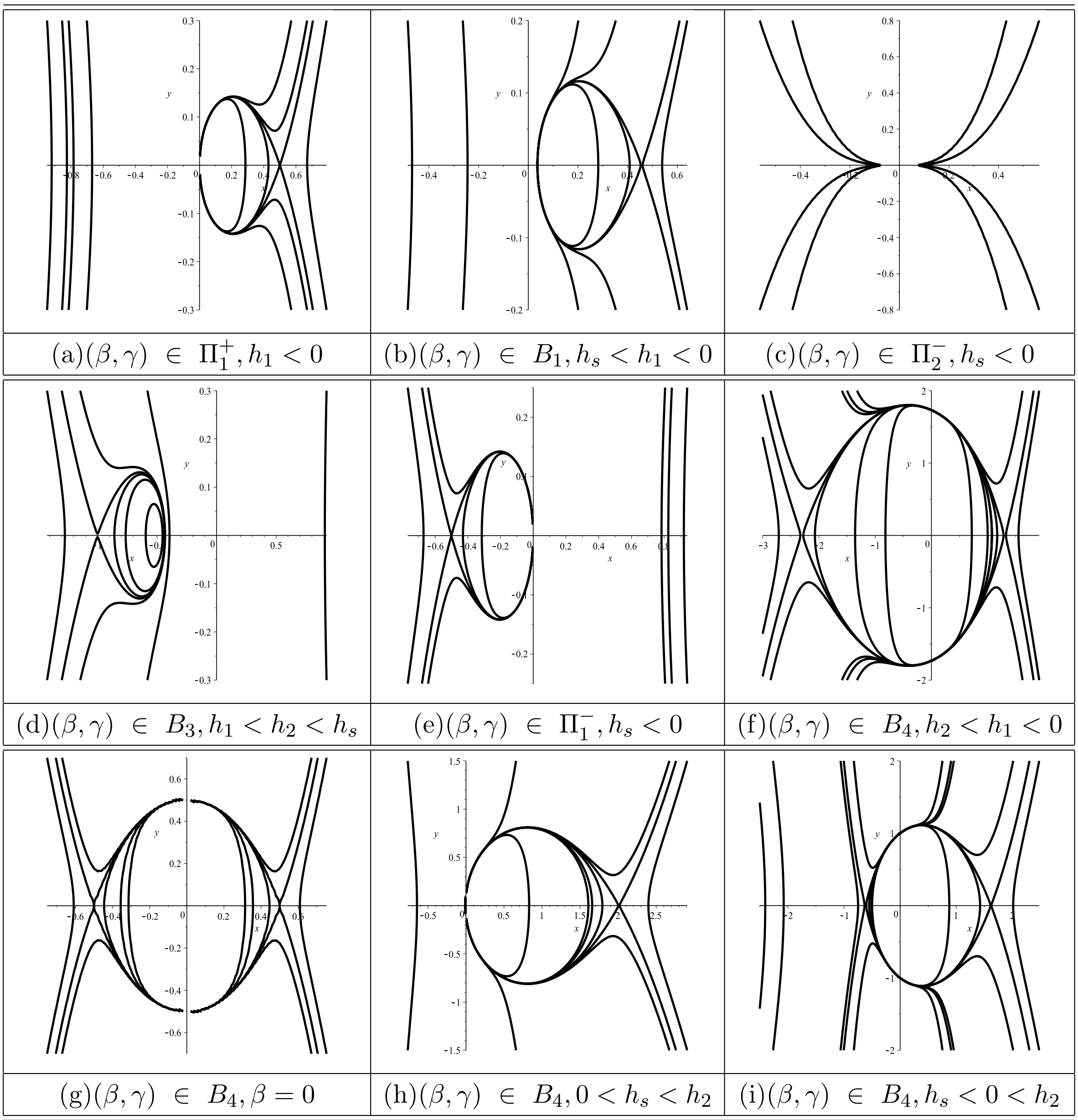

(a)$(\beta, \gamma) \in \Pi_1^+, h_1 < 0$ (b)$(\beta, \gamma) \in B_1, h_s < h_1 < 0$ (c)$(\beta, \gamma) \in \Pi_2^-, h_s < 0$

(d)$(\beta, \gamma) \in B_3, h_1 < h_2 < h_s$ (e)$(\beta, \gamma) \in \Pi_1^-, h_s < 0$ (f)$(\beta, \gamma) \in B_4, h_2 < h_1 < 0$

(g)$(\beta, \gamma) \in B_4, \beta = 0$ (h)$(\beta, \gamma) \in B_4, 0 < h_s < h_2$ (i)$(\beta, \gamma) \in B_4, h_s < 0 < h_2$

FIGURE 2. Bifurcations of phase portraits of system (6) in the (ϕ, y)-phase plane when $\alpha > 0$ and $n = 2m$

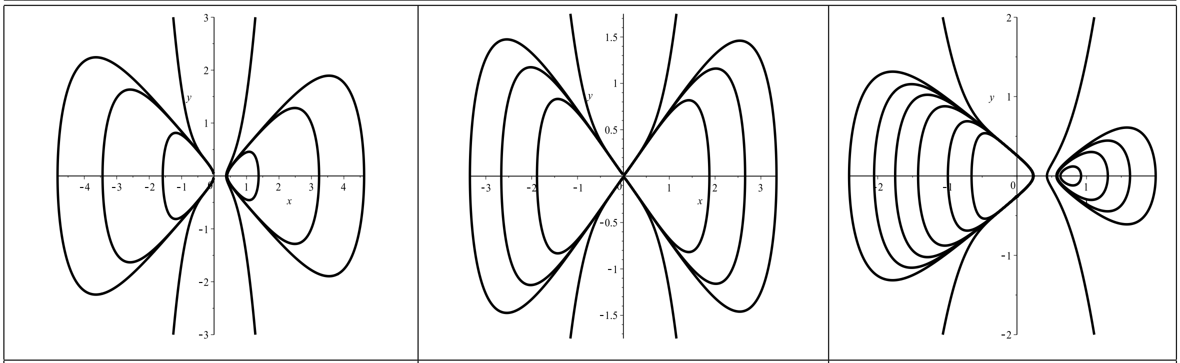

(a)$(\beta,\gamma) \in \Pi_1^+, 0 < h_1$ | (b)$(\beta,\gamma) \in B_1, \Delta = 0, 0 < h_s$ | (c)$(\beta,\gamma) \in \Pi_1^-,\ 0 < h_1$

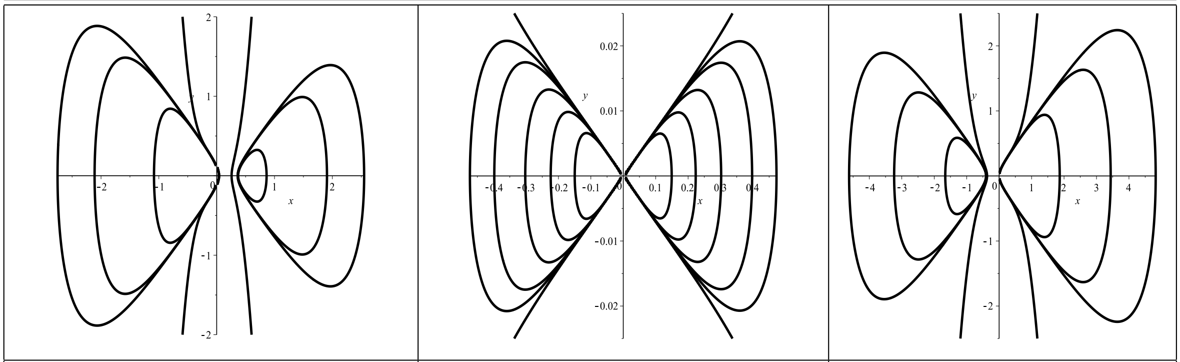

(d)$(\beta,\gamma) \in B_2, h_s < 0 < h_1$ | (e)$(\beta,\gamma) \in \Pi_2^+, \Delta < 0$ | (f)$(\beta,\gamma) \in \Pi_1^-, 0 < h_s$

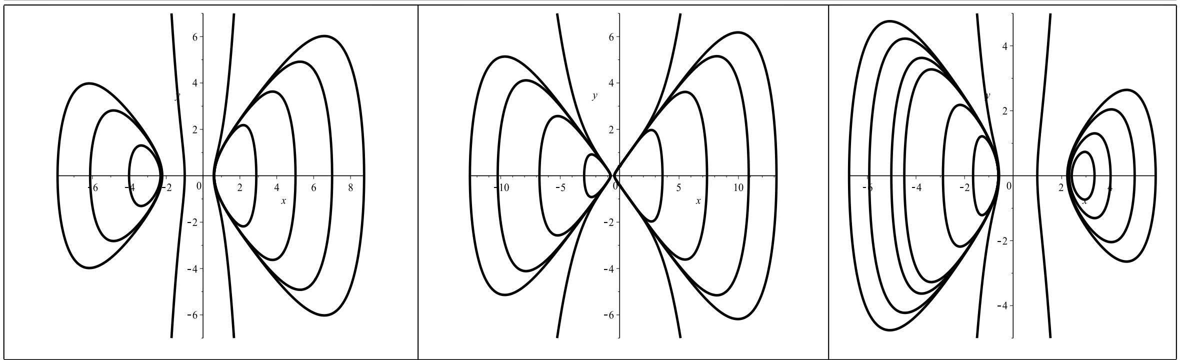

(g)$(\beta,\gamma) \in B_4, Y_s < 0, h_1 < 0$ | (h)$(\beta,\gamma) \in B_4, Y_s > 0,$ | (i)$(\beta,\gamma) \in B_4, Y_s < 0.$

FIGURE 3. Bifurcations of phase portraits of system (6) in the (ϕ, y)-phase plane when $\alpha < 0$ and $n = 2m$

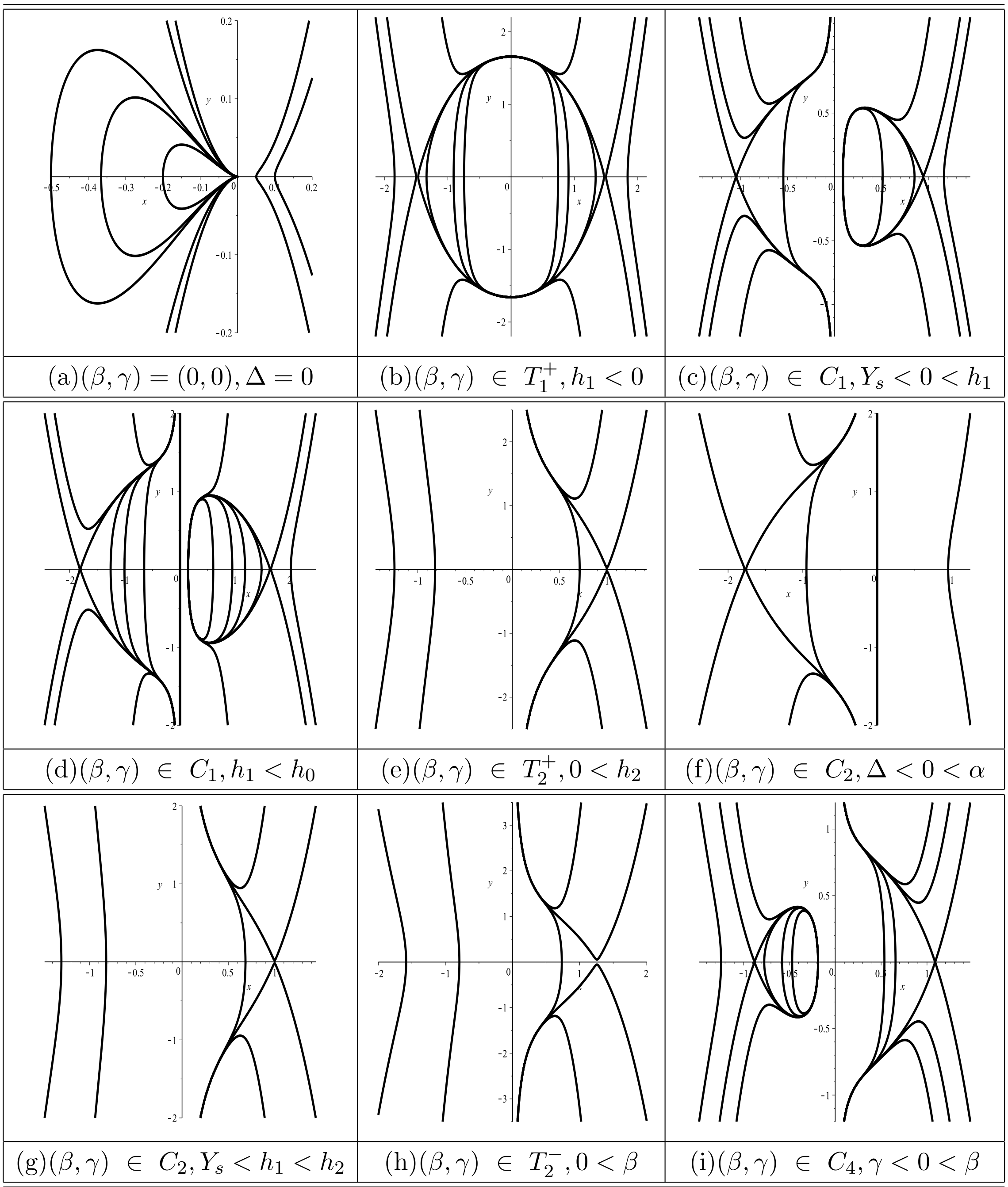

(a)$(\beta,\gamma) = (0,0), \Delta = 0$ (b)$(\beta,\gamma) \in T_1^+, h_1 < 0$ (c)$(\beta,\gamma) \in C_1, Y_s < 0 < h_1$

(d)$(\beta,\gamma) \in C_1, h_1 < h_0$ (e)$(\beta,\gamma) \in T_2^+, 0 < h_2$ (f)$(\beta,\gamma) \in C_2, \Delta < 0 < \alpha$

(g)$(\beta,\gamma) \in C_2, Y_s < h_1 < h_2$ (h)$(\beta,\gamma) \in T_2^-, 0 < \beta$ (i)$(\beta,\gamma) \in C_4, \gamma < 0 < \beta$

FIGURE 4. Bifurcations of phase portraits of system (6) in the (ϕ, y)-phase plane when $\alpha > 0$ and $n = 2m+1$

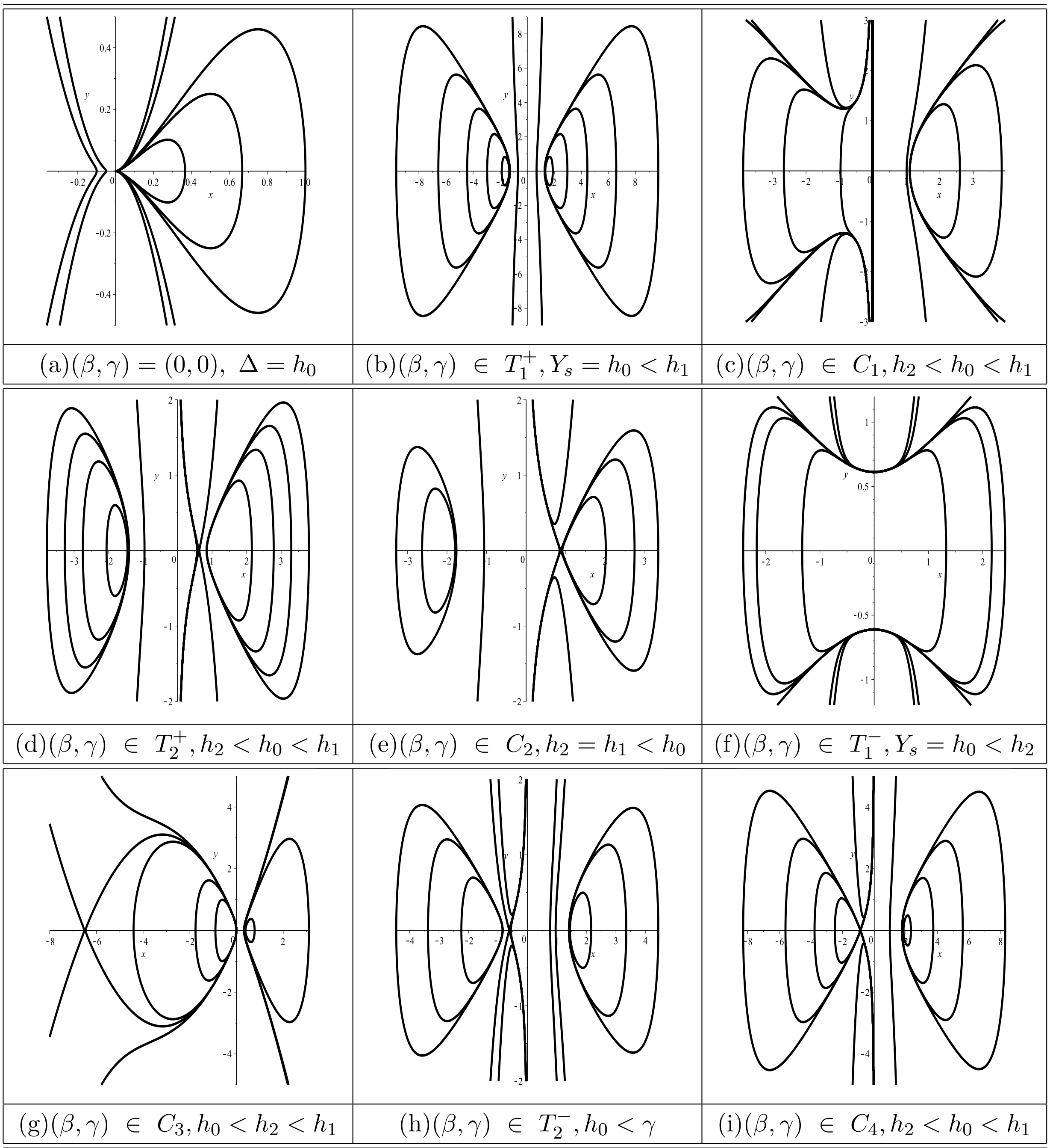

FIGURE 5. Bifurcations of phase portraits of system (6) in the (ϕ, y)-phase plane when $\alpha<0$ and $n=2m+1$

3. Parametric representation of exact wave solutions of equation (3) when $n = 2$.

In this section, we shall consider all possible exact explicit parametric representations for all bounded functions $\phi(\xi) = \sqrt{\varphi(\xi)}$ determined by system (6). Then, we obtain corresponding traveling wave solutions of equation (3) in different parameter regions of the (α, β, γ)- parameter space for $n = 2$.

We see from equation (7) and the first equation of system (6) in calculating the exact explicit parametric representation of the solutions one has:

$$\left(2\sqrt{2}\right)\xi = \int_{\phi_0}^{\phi} \frac{2d\phi}{\sqrt{\alpha\left(-\frac{1}{4}\phi^2 + \frac{\beta}{5}\phi - \frac{\gamma}{6}\right) - h\phi^6}} = \int_{\varphi_0}^{\varphi} \frac{d\varphi}{\sqrt{\alpha\left(-\frac{1}{4}\varphi^2 + \frac{\beta}{5}\varphi^{\frac{3}{2}} - \frac{\gamma}{6}\varphi\right) - h\varphi^4}}, \quad (10)$$

Then from equation (10), we may obtain the parametric representations of solutions of system (6) and equation (3).

3.1. ***Parametric representation of exact wave solutions of equation (3) when*** $\alpha < 0$.. **1. The case of** $(\beta, \gamma) \in \Pi_1^+, h_1 < h_0$**.** (see Fig.2 (a)).

(i) In this case, $\varphi_m = h_0$. Corresponding to the homoclinic orbits to the saddle point $A_2(\phi_2, 0)$, enclosing the equilibrium point $A_1(\phi_1, 0)$ given by $H_2(\phi, y) = h_1$. Using the first equation of system (6), we have

$$\int_0^{\varphi} \frac{d\varphi}{(\varphi_2 - \varphi)\sqrt{(\varphi - \varphi_l)\varphi}} = \left(2\sqrt{2}\right)\xi.$$

where, $\varphi_l < 0\varphi_1 < \varphi_2 < \varphi_L$. It follows the exact solutions of equation (6):

$$\varphi(\xi) = \varphi_2 - \frac{2(\varphi_2 - \varphi_l)\varphi_2}{(\varphi_l - 2\varphi_2) - \varphi_l \cosh(\omega_0 \xi)}, \quad (11)$$

where $\omega_0 = 2\sqrt{2\varphi_2(\varphi_2 - \varphi_l)}$.

Thus, we obtain the exact solitary wave solution of equation (3) as follows (see Fig. 6(a)):

$$u(x,t) = \left(\varphi_2 - \frac{2(\varphi_2 - \varphi_l)\varphi_2}{(\varphi_l - 2\varphi_2) - \varphi_l \cosh(\omega_0 \xi)}\right)^{\frac{1}{2}}. \quad (12)$$

(ii) Corresponding to the level curve defined by $H_2(\phi, y) = h$ where $h \in (h_1, h_0)$ there exists a periodic orbit to the singular straight line $\phi = 0$, enclosing the equilibrium point $A_1(\phi_1, 0)$. Using the first equation of system (6), we have

$$\int_0^{\varphi} \frac{d\varphi}{\sqrt{(\varphi - \varphi_l)\varphi(r_1 - \varphi)(\varphi_L - \varphi)}} = \left(2\sqrt{2}\right)\xi.$$

where $\phi_l < 0 < r_1 < \phi_L$. It follows the exact solutions of equation (6):

$$\varphi(\xi) = \varphi_l\left(1 - \frac{1}{1 - \alpha_1^2 \mathrm{sn}^2(\omega_1 \xi, k_1)}\right), \quad (13)$$

where $\omega_1 = \sqrt{2\phi_L(r_1 - \phi_l)}$, $\alpha_1^2 = \frac{r_1}{r_1-\phi_l}$, $k_1^2 = \frac{(\phi_L-\phi_l)r_1}{(r_1-\phi_l)\phi_L}$, $\mathrm{sn}(\cdot, k_1)$, $\mathrm{cn}(\cdot, k_1)$, and $\mathrm{dn}(\cdot, k)$ are Jacobin elliptic functions and $\Pi(\cdot, \cdot, k_1)$ is the normal elliptic integral of the third kind (see [16]).

Thus, we obtain the exact periodic wave solution of equation (3) as follows(see Fig. 6(b)):

$$u(x,t) = \sqrt{\varphi_l}\left(1 - \frac{1}{1 - \alpha_1^2 \mathrm{sn}^2(\omega_1(x-ct), k_1)}\right)^{\frac{1}{2}}. \tag{14}$$

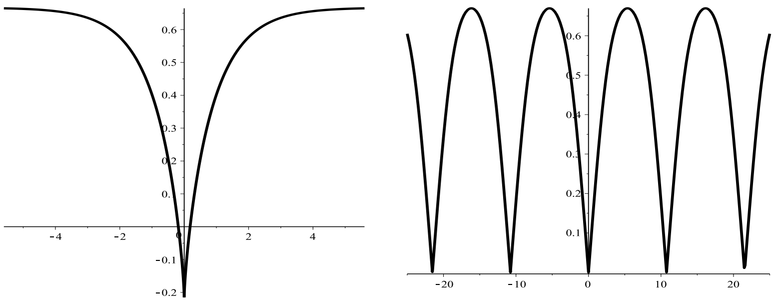

(a) solitary wave. (b) Periodic wave.

FIGURE 6. Profile of solitary waves, periodic waves and compacton of system (6) when $(\beta, \gamma) \in \Pi_1^+$ and $\alpha > 0$

Corresponding to open curves passing through $(\varphi_l, 0)$ and $(\varphi_L, 0)$ we have the following compacton solution of equation (3), respectively(see Fig. 7(a) and 7(b)):

$$u_l(x,t) = \left(\frac{\varphi_l}{1 - \left(\frac{\phi_L-\phi_l}{\phi_L}\right)\mathrm{sn}^2(\omega_1(x-ct), k_1)}\right)^{\frac{1}{2}}. \tag{15}$$

$$u_L(x,t) = \left(r_1 + \frac{\varphi_L - r_1}{1 - \left(\frac{\phi_L-\phi_l}{r_1-\phi_l}\right)\mathrm{sn}^2(\omega_1(x-ct), k_1)}\right)^{\frac{1}{2}}. \tag{16}$$

(iii) Corresponding to the level curve defined by $H_2(\phi, y) = h$ where $h \in (-\infty, h_1)$ and $h \in (h_0, +\infty)$ has a family of uncountably infinite many open curve tending to the singular straight line $\phi = 0$, passing through $E_0(0, 0)$.

2. The case of $(\beta, \gamma) \in B_1$, $\Delta = 0$, $h_0 < h_s < +\infty$. (see Fig.2 (b)).

(i) For $h \in (h_1, h_2,)$ the level curve defined by $H_2(\phi, y) = h$, there exists a family of periodic orbits enclosing the equilibrium point $A_1(\phi_1, 0)$. Thus, from equation (10) we have

$$\int_{r_1}^{\varphi} \frac{d\varphi}{\sqrt{(\varphi - r_4)(\varphi - r_3)(r_2 - \varphi)(r_1 - \varphi)}} = \left(2\sqrt{2}\right)\xi.$$

where, $r_1 > r_2 > r_3 > r_4$.

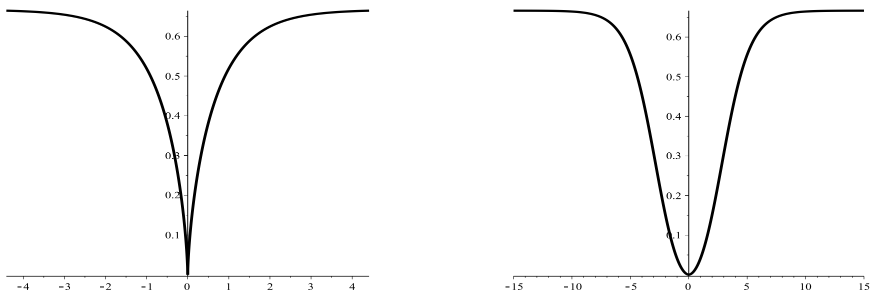

(a) Compacton wave (left family) (b) Compacton wave (right family).

FIGURE 7. Profile of compacton wave of system (6) when $(\beta,\gamma) \in \Pi_1^+$ and $\alpha > 0$

It follows the exact solutions of equation (6):

$$\varphi(\xi) = r_4 + \frac{r_3 - r_4}{1-\alpha_2^2\mathrm{sn}^2(\omega_2\xi, k_2)}, \tag{17}$$

where $\omega_2 = \sqrt{2(r_1-r_3)(r_2-r_4)}$, $\alpha_2^2 = \frac{r_2-r_3}{r_2-r_4}$, $k_2^2 = \frac{(r_2-r_3)(r_1-r_4)}{(r_2-r_4)(r_2-r_4)}$

Thus, we obtain the exact periodic solution of equation (3) as follows:

$$u(x,t) = \left(r_4 + \frac{r_3 - r_4}{1-\alpha_2^2\mathrm{sn}^2(\omega_2(x-ct), k_2)}\right)^{\frac{1}{2}}. \tag{18}$$

(ii) In this case $\phi_l < 0 < \phi_m < \phi_1 < \phi_2 < \phi_L$.

For the level curve defined by $H_2(\phi, y) = h_2$, there exists a homoclinic orbit to the saddle point $A_2(\phi_2, 0)$ enclosing the equilibrium point $A_1(\phi_1, 0)$ to the right of the singular line $\phi = 0$. Using the first equation of (6) we have:

$$\int_{\varphi_m}^{\varphi} \frac{d\varphi}{(\varphi_2-\varphi)\sqrt{(\varphi-\varphi_l)\varphi(\varphi-\varphi_m)}} = \left(2\sqrt{2}\right)\xi.$$

It follows the exact solutions of equation (6):

$$\varphi(\xi) = \varphi_2 - \frac{2(\varphi_2-\varphi_l)(\varphi_2-\varphi_m)}{(\varphi_m-\varphi_l)\cosh(\omega_3\xi) + (\varphi_m+\varphi_l)}, \tag{19}$$

where $\omega_3 = 2\sqrt{2(\varphi_2-\varphi_l)(\varphi_2-\varphi_m)}$.

Thus, we obtain the exact solitary wave solution of equation (3) as follows:

$$u(x,t) = \left(\varphi_2 - \frac{2(\varphi_2-\varphi_l)(\varphi_2-\varphi_m)}{(\varphi_m-\varphi_l)\cosh(\omega_3\xi) + (\varphi_m+\varphi_l)}\right)^{\frac{1}{2}}. \tag{20}$$

3. The case of $(\beta,\gamma) \in \Pi_2^-$, $h_s < h_0$**.** (see Fig.2 (c)).

In this case $\varphi_2 = -\varphi_1$. For $h = h_s$, the level curve defined by $H_2(\phi, y) = h$, there exists a cusp at the point $A_1(\phi_1, 0)$ and $A_2(\phi_2, 0)$. Thus, we obtain the exact solution of equation

(6) as follows:

$$\varphi(\xi) = \varphi_2^2 - \exp(\omega_4 \xi), \tag{21}$$

where $\omega_4 = 4\sqrt{2\varphi_2}$.

Hence, we obtain the exact solution of equation (3) as follows:

$$u(x,t) = \left[\varphi_2^2 - \exp(\omega_4(x - ct))\right]^{\frac{1}{2}}. \tag{22}$$

4. The case of $(\beta, \gamma) \in B_3,\ h_1 < h_2 < h_s$**.** (see Fig.2 (d)).

(i) For $h = h_2$ the level curve defined by $H_2(\phi, y) = h$, there exists a homoclinic orbit at $A_1(\phi_1, 0)$ enclosing $A_2(\phi_2, 0)$. Using the first equation of (6) we have:

$$\int_{\varphi}^{\varphi_M} \frac{d\varphi}{(\varphi - \varphi_1)\sqrt{(\varphi_M - \varphi)(\varphi_L - \varphi)}} = \left(2\sqrt{2}\right)\xi.$$

where, $\varphi_l < \varphi_1 < \varphi_2 < \varphi_L$ It follows the exact solutions of equation (6):

$$\varphi(\xi) = \varphi_1 + \frac{2(\varphi_M + \varphi_1)(\varphi_L + \varphi_1)}{(\varphi_L - \varphi_M)\cosh(\omega_5 \xi) - (\varphi_M + \varphi_L) - 2\varphi_1}, \tag{23}$$

where $\omega_5 = 2\sqrt{2(\varphi_M + \varphi_1)(\varphi_L + \varphi_1)}$.

Thus, we obtain the exact solitary wave solution of equation (3) as follows:

$$u(x,t) = \left(\varphi_1 + \frac{2(\varphi_M + \varphi_1)(\varphi_L + \varphi_1)}{(\varphi_L - \varphi_M)\cosh(\omega_5(x - ct)) - (\varphi_M + \varphi_L) - 2\varphi_1}\right)^{\frac{1}{2}}. \tag{24}$$

(ii) Specially, taking $\varphi_M = 0$, of Fig. 2(e), we have the exact solitary wave solution of equation (3) as follows:

$$u(x,t) = \left(\varphi_1 + \frac{2\varphi_1(\varphi_1 - \varphi_L)}{(\varphi_L - 2\varphi_1) - (\varphi_L)\cosh(\omega_5(x - ct))}\right)^{\frac{1}{2}}. \tag{25}$$

5. The case of $(\beta, \gamma) \in B_4,\ \beta = h_0,\ \gamma < 0$**.** (see Fig.2 (g)).

For $h \in (h_0, h_1)$, system (6) has four heteroclinic orbits connecting to the saddle points $A_1(\phi_1, 0)$ and $A_2(\phi_2, 0)$ passing through $Q_1(0, -Y_s)$ and $Q_2(0, Y_s)$. Then, from equation (10), we have

$$\int_{\varphi_0}^{\varphi} \frac{d\varphi}{(\varphi - \varphi_1)(\varphi_2 - \varphi)} = \left(2\sqrt{2}\right)\xi.$$

where, $\varphi_0 \in (\varphi_1, \varphi_2)$. It follows the exact solutions of equation (6):

$$\varphi(\xi) = \varphi_2 - \frac{\varphi_2 - \varphi_1}{1 - \exp((\varphi_2 - \varphi_1)\xi)}. \tag{26}$$

Thus, we obtain kink and anti-kink wave solution of equation (3) as follows:

$$u(x,t) = \left(\varphi_2 - \frac{\varphi_2 - \varphi_1}{1 - \exp((\varphi_2 - \varphi_1)\xi)}\right)^{\frac{1}{2}}. \tag{27}$$

6. The case of $(\beta, \gamma) \in B_4,\ h_s < h_0 < h_2$**.** (see Fig.2 (i)).

In Fig. 2(i), the level curves defined by $H_2(\phi, y) = h$ for $h \in (h_1, h_0)$, contain two stable manifolds and two unstable manifolds of the saddle point at $A_1(\phi_1, 0)$, where $\phi_1 = -\frac{14}{5}$ The function $\varphi(\xi)$ in the left two manifolds tends asymptotically to the singular straight line $\phi = 0$ as $|y| \to \infty$. So, corresponding to the left stable manifold and unstable manifold about the saddle point $A_1(\phi_1, 0)$, one has the following two parametric representations of the solutions of system (6):

$$\varphi(\xi) = \varphi_1 + \frac{4(\varphi_1 - \varphi_l)(\varphi_L - \varphi_1)P}{P^2\exp(\pm\omega_6\xi) + (\varphi_L - \varphi_l)^2\exp(\mp\omega_6\xi) - 2(\varphi_L + \varphi_l - 2\varphi_1)}, \tag{28}$$

where $\varphi_l < \varphi_1 < 0 < \varphi_L,\ P = \varphi_L - \varphi_l,\ \omega_6 = \sqrt{8(\varphi_1 - \varphi_l)(\varphi_L - \varphi_1)},$
$\xi \in (-\infty, \infty)$.

Thus, we obtain the exact compacton wave solution of equation (3) as follows:

$$u(x,t) = \left(\varphi_1 + \frac{4(\varphi_1 - \varphi_l)(\varphi_L - \varphi_1)P}{P^2\exp(\pm\omega_6(x-ct)) + (\varphi_L - \varphi_l)^2\exp(\mp\omega_6(x-ct)) - 2(\varphi_L + \varphi_l - 2\varphi_1)}\right)^{\frac{1}{2}}. \tag{29}$$

3.2. ***Parametric representation of exact wave solutions of equation (3) when*** $\alpha < 0$**.** In this section, we give some exact explicit parametric representations of the traveling wave solutions such as solitary solutions, compacton solutions, periodic cusp wave solutions and periodic traveling wave solutions.

1. The case of $(\beta, \gamma) \in \Pi_1^+,\ h_0 < h_1$**.** (see Fig. 3(a)).

For the level curves defined by $H_2(\phi, y) = 0$, there exists a family of a periodic orbits to the right and left of the singular straight line $\phi = 0$. Thus, corresponding to the left family of periodic orbit equation (10) becomes:

$$\int_{r_3}^{\varphi} \frac{d\varphi}{\sqrt{(\varphi - r_3)\varphi(r_2 - \varphi)(r_1 - \varphi)}} = \left(2\sqrt{2}\right)\xi.$$

where, $r_3 < 0 < r_2 < r_1$. It follows the exact solutions of equation (6):

$$\varphi_l(\xi) = r_1 + \frac{r_3 - r_1}{1 - \alpha_3^2\mathrm{sn}^2(\omega_7\xi, k_3)}, \tag{30}$$

where, $\omega_7 = \sqrt{8r_1(r_2 - r_3)},\ \alpha_3^2 = \frac{r_3}{r_1},\ k_3^2 = \frac{r_3(r_2 - r_1)}{r_1(r_2 - r_3)}$

Thus, we obtain a periodic wave solution of equation (3) as follows (see Fig.8(a)):

$$u_l(x,t) = \left(r_1 + \frac{r_3 - r_1}{1 - \alpha_3^2\mathrm{sn}^2(\omega_7(x-ct), k_3)}\right)^{\frac{1}{2}}. \tag{31}$$

Corresponding to the right family of periodic orbit we have an exact solutions of equation (3) as follows (see Fig.8(b)):

$$u_r(x,t) = \left(\frac{r_2}{1 - \alpha_4^2\mathrm{sn}^2(\omega_7(x-ct), k_3)}\right)^{\frac{1}{2}}. \tag{32}$$

where $\alpha_4^2 = \frac{r_1 - r_2}{r_1}$.

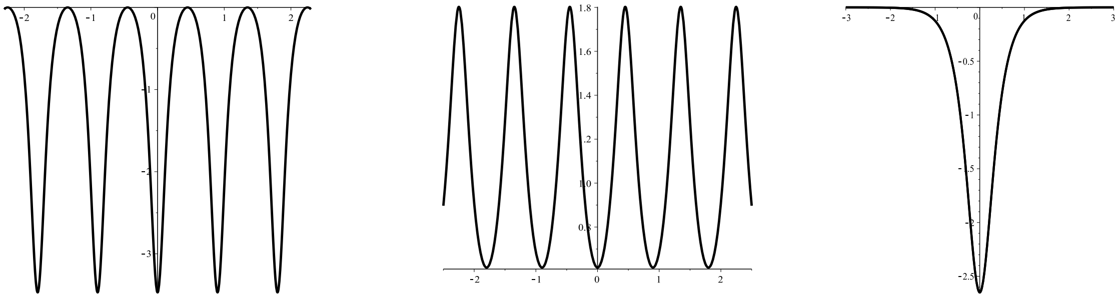

(a)Periodic wave (left-family) (b)Periodic wave (right-family) (c)Solitary Wave

FIGURE 8. Profile of periodic wave families and solitary wave of system (6) when $\alpha < 0$

2. The case of $(\beta, \gamma) \in B_1,\ \Delta = 0,\ h_0 < h_s < +\infty$**.** (see Fig. 3(b) & 3(e)).

Corresponding to the right homoclinic orbit and left homoclinic orbit to the equilibrium point $A_0(0,0)$, we see from equation (10) that we have the exact solutions of equation (6), respectively, as follows:

$$\varphi_r(\xi) = \frac{2\varphi_M|\varphi_m|}{(\varphi_M - \varphi_m)\cosh(\omega_8\xi) - (\varphi_M + \varphi_m)} \tag{33}$$

and

$$\varphi_l(\xi) = \frac{-2\varphi_M|\varphi_m|}{(\varphi_M - \varphi_m)\cosh(\omega_8\xi) + (\varphi_M + \varphi_m)}, \tag{34}$$

where $\omega_8 = \sqrt{8\varphi_M|\varphi_m|}$.

Equation (33) and (34) give rise to the exact solitary wave solutions of equation (3) as follows (see Fig.8(c)): for $n > 1$,

$$u_r(x,t) = \left(\frac{2\varphi_M|\varphi_m|}{(\varphi_M - \varphi_m)\cosh(\omega_8(x-ct)) - (\varphi_M + \varphi_m)}\right)^{\frac{1}{2}}. \tag{35}$$

and for n is a odd number,

$$u_l(x,t) = \left(\frac{-2\varphi_M|\varphi_m|}{(\varphi_M - \varphi_m)\cosh(\omega_8(x-ct)) + (\varphi_M + \varphi_m)}\right)^{\frac{1}{2}}. \tag{36}$$

3. The case of $(\beta, \gamma) \in \Pi_1^-,\ h_0 < h_1$**.** (see Fig. 3(c), 3(d), 3(f), 3(g) & 3(i)).

Corresponding to the curves defined by $H_2(\phi, y) = h,\ h \in (h_2, h_1)$ in (7), equation (6) has two families of periodic solutions. Now, (10) can be written as

$$\int_{\varphi_d}^{\varphi} \frac{d\varphi}{\sqrt{(\varphi - \varphi_d)(\varphi_c - \varphi)(\varphi_b - \varphi)(\varphi_a - \varphi)}} = \left(2\sqrt{2}\right)\xi.$$

where, $\varphi_d < \varphi_c < \varphi_b < \varphi_a$. for the family of periodic orbits shown on the left-hand side of Figure 3(c), and

$$\int_{\varphi_b}^{\varphi} \frac{d\varphi}{\sqrt{(\varphi-\varphi_d)(\varphi-\varphi_c)(\varphi-\varphi_b)(\varphi_a-\varphi)}} = \left(2\sqrt{2}\right)\xi.$$

for the family of periodic orbits shown on the right-hand side of Figure 3(c). Thus, we have parametric representations for the two families of periodic solutions of equation (6), respectively as follows:

$$\varphi_l(\xi) = \varphi_d + \frac{(\varphi_d-\varphi_a)\alpha_l^2 \mathrm{sn}^2(\omega_9\xi, k_4)}{1-\alpha_l^2 \mathrm{sn}^2(\omega_9\xi, k_4)}, \tag{37}$$

and

$$\varphi_r(\xi) = \varphi_b + \frac{(\varphi_b-\varphi_c)\alpha_r^2 \mathrm{sn}^2(\omega_9\xi, k_4)}{1-\alpha_r^2 \mathrm{sn}^2(\omega_9\xi, k_4)}, \tag{38}$$

where $\omega_9 = \sqrt{8(\varphi_a-\varphi_c)(\varphi_b-\varphi_d)}$, $k_4 = \sqrt{\frac{(\varphi_a-\varphi_b)(\varphi_c-\varphi_d)}{(\varphi_a-\varphi_c)(\varphi_b-\varphi_d)}}$, $\alpha_l = \sqrt{\frac{\varphi_c-\varphi_d}{\varphi_a-\varphi_c}}$, $\alpha_r = \sqrt{\frac{\varphi_a-\varphi_b}{\varphi_a-\varphi_c}}$.

Thus, we have the following exact periodic traveling wave solution corresponding to (37) and (38) of equation (3) respectively:

$$u_l(x,t) = \left(\varphi_d + \frac{(\varphi_d-\varphi_a)\alpha_l^2 \mathrm{sn}^2(\omega_9\xi, k_4)}{1-\alpha_l^2 \mathrm{sn}^2(\omega_9(x-ct), k_4)}\right)^{\frac{1}{2}}. \tag{39}$$

and

$$u_r(x,t) = \left(\varphi_b + \frac{(\varphi_b-\varphi_c)\alpha_r^2 \mathrm{sn}^2(\omega_9\xi, k_4)}{1-\alpha_r^2 \mathrm{sn}^2(\omega_9\xi, k_4)}\right)^{\frac{1}{2}}. \tag{40}$$

Theorem 1

Depending on the changes of system parameters $\alpha,\ \beta,\ \gamma$, the bifurcations of phase portraits of system (6) for $n = 2$, when $\alpha\ \in \mathbb{R}$ are shown in Fig. 1 (a), Fig.2 and Fig.3.

(i) Equation (3) has exact periodic wave solutions given by (12), (14), (18), (31), (32), (39) and (40).

(ii) Equation (3) has exact kink and anti-kink solutions given by (27).

(iii) Equation (3) has exact compacton solutions given by (15), (16), (22) and (29).

(iv) Equation (3) has exact solitary wave solutions given by (20), (24), (25), (35) and (36).

Theorem 2: Suppose that $n = 2m,\ m \in \mathbb{Z}^+$ and see figure 2 and figure 3.

(1) For $(\beta,\gamma)\ \in\ \Pi_1^+$. When $\alpha > 0$, equation (3) has a smooth solitary wave solutions with valley form for $h = h_1$, and has a family of uncountably infinite many smooth periodic solutions for $h\ \in\ (h_1, h_0)$. Corresponding to the level curve defined by $H_2(\phi, y) = h$ where $h\ \in\ (-\infty, h_1)$ and $h\ \in\ (h_0, +\infty)$ has a family of uncountably infinite many open curve tending to the singular straight line $\phi = 0$, passing through $E_0(0,0)$. And when $\alpha < 0$, equation (3) has a family of uncountably infinite many periodic solutions for $h = h_0$, and

their amplitudes tend to ∞ for $h \to 0$.

(2) For $(\beta, \gamma) \in B_1$. When $\alpha > 0$, equation (3) has a smooth solitary wave solutions with valley form for $h = h_2$, at $A_1(\phi_1, 0)$ and has a family of uncountably infinite many smooth periodic solutions for $h \in (h_1, h_2)$. And when $\alpha < 0$, equation (3) has a family of uncountably infinite many smooth periodic solutions for $h \in (h_2, 0)$ and if $H(\phi_1, 0) = h$ (here $A_2(\phi_2, 0)$ is the saddle point) defined by (6) has a zero ϕ^* satisfying $0 < \phi_1 < \phi^*$, equation (3) has a smooth solitary wave solutions with peak form for $h = h_2$ and a family of uncountably infinite many smooth periodic solutions for $h \in (h_2, h_1)$.

(3) For $(\beta, \gamma) \in \Pi_2^-$. When $\alpha > 0$, equation (3) has a cusp solitary wave solutions with peak form for $h = h_s$, and has a family of uncountably infinite many smooth periodic solutions for $h \in (h_2, h_1)$.

(4) For $(\beta, \gamma) \in B_4$. When $\alpha < 0$, equation (3) has two families of uncountably infinite many smooth periodic solutions for $h \in (h_1, 0)$. And, when $\alpha > 0$, equation (3) has two stable manifolds and two unstable manifolds of the saddle point at $A_1(\phi_1, 0)$ tending asymptotically to the singular straight line $\phi = 0$ as $|y| \to \infty$ for $h \in (h_1, h_0)$.

4. Parametric representation of exact wave solutions of equation (3) when $n = 3$.

We see from equation (7) and the first equation of system (6) and system (8) in calculating the exact explicit parametric representation of the solutions one has:

$$\left(2\sqrt{2}\right)\xi = \int_{\phi_0}^{\phi} \frac{2d\phi}{\sqrt{\alpha\left(-\frac{1}{6}\phi^2 + \frac{\beta}{8}\phi - \frac{\gamma}{9\phi}\right) - h\phi^8}} = \int_{\varphi_0}^{\varphi} \frac{d\varphi}{\sqrt{\alpha\left(-\frac{1}{6}\varphi^2 + \frac{\beta}{8}\varphi - \frac{\gamma}{9}\varphi^{\frac{1}{2}}\right) - h\varphi^5}}, \tag{41}$$

Then from equation (10), we may obtain the parametric representations of solutions of system (6).

4.1. ***Parametric representation of exact wave solutions of equation (3) when $\alpha > 0$.***

In this section, we give some exact explicit parametric representations of the traveling wave solutions of equation (3).

1. The case of $(\beta, \gamma) = (0, 0),\ \Delta = 0,\ h_1 < h_0$**.** (see Fig. 4(a)).

Corresponding to the curves defined by $H_3(\phi, y) = h,\ h \in (h_1, h_0)$ (see Fig. 4(a)), we have from equation (7) that $y^2 = 8(\varphi - \varphi_m)\varphi^3(\varphi_L - \varphi)$, where $\varphi_m < 0 < \varphi_L$. Equation (6) has a homoclinic orbit to the cusp point $A_0(0, 0)$. Then from equation (41) we have

$$\int_{\varphi_m}^{\varphi} \frac{d\varphi}{\varphi\sqrt{(\varphi - \varphi_m)\varphi(\varphi_L - \varphi)}} = \left(2\sqrt{2}\right)\xi.$$

It follows the exact solutions of equation (6):

$$\varphi(\xi) = \varphi_m \mathrm{cn}^2(\Omega_1 \xi, k_5), \tag{42}$$

where, $\Omega_1 = \sqrt{2(\varphi_L - \varphi_m)}$, $k_5^2 = \left(1 - \frac{\varphi_L}{\varphi_m}\right)^{-1}$.

Thus, we obtain a solitary wave solution of equation (3) as follows (see Fig 9(a)):

$$u(x,t) = \sqrt{\varphi_m}\mathrm{cn}(\Omega_1(x-ct), k_5). \tag{43}$$

Corresponding to the open arch curve to the right of the singular straight line $\phi = 0$, we have from equation (41) that:

$$\int_{\varphi_L}^{\varphi} \frac{d\varphi}{\varphi\sqrt{(\varphi - \varphi_m)\varphi(\varphi - \varphi_L)}} = \left(2\sqrt{2}\right)\xi.$$

It follows the exact solutions of equation (6):

$$\varphi(\xi) = \varphi_L \mathrm{nc}^2(\Omega_1 \xi, k_6), \tag{44}$$

where, $k_6^2 = \frac{\varphi_m}{\varphi_L}$.

Thus, we obtain a compacton solution of equation (3) as follows (see Fig 9(b)):

$$u(x,t) = \sqrt{\varphi_L}\mathrm{nc}(\Omega_1(x-ct), k_6). \tag{45}$$

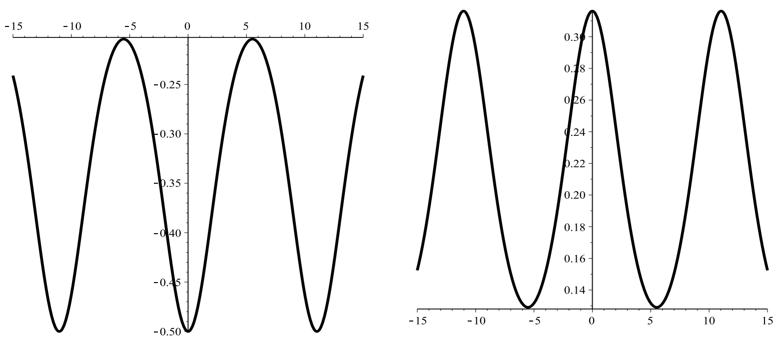

(a) Solitary wave. (b) Compacton wave.

FIGURE 9. Profile of solitary waves and compacton waves of system (6) when $(\beta,\gamma) \in T_1^+$ when $\alpha < 0$

2. The case of $(\beta,\gamma) \in T_1^+$, $h_1 < h_0$**.** (see Fig. 4(b)).

In this case, $\varphi_1 < 0 < \varphi_2 < \varphi_L$. Corresponding to the level curve defined by $H_3(\phi, y) = h_1$, there exists a heteroclinic orbit connecting the equilibrium points $A_1(\phi_1, 0)$ and $A_2(\phi_2, 0)$. Moreover we see from (7) that the two arch curve connecting the equilibrium points $Q_1(0, -Y_s)$

and $Q_2(0, Y_s)$ in the left and right side of the straight line $\phi = 0$ enclosing the origin have the exact solution of equation (6):

$$\varphi(\xi) = \varphi_L - \Psi_1 \left(\frac{1 + \exp(\Omega_2 \xi)}{1 - \exp(\Omega_2 \xi)} \right)^2, \tag{46}$$

where, $\Psi_1 = \varphi_L - \varphi_1,\ \Omega_2 = 4\varphi_2\sqrt{2\Psi_1}$.

Hence, we obtain a kink and anti-kink wave solution of equation (3) as follows:

$$u(x,t) = \left[\varphi_L - \Psi_1 \left(\frac{1 + \exp(\Omega_2(x - ct))}{1 - \exp(\Omega_2(x - ct))} \right)^2 \right]^{\frac{1}{2}}. \tag{47}$$

3. The case of $(\beta, \gamma) \in C_1,\ h_0 < h_1$**.** (see Fig. 4(c), 4(d) & 4(i)).

(i) Corresponding to the curves defined by $H_3(\phi, y) = h_0$ in (7), equation (6) has a periodic orbit enclosing the equilibrium point $A_2(\phi_2, 0)$. We obtain from equation (41) that:

$$\int_{r_3}^{\varphi} \frac{d\varphi}{(\varphi - \varphi_1)\sqrt{(\varphi - r_3)(r_2 - \varphi)(r_1 - \varphi)}} = \left(2\sqrt{2}\right)\xi.$$

where, $r_3 < 0 < r_2 < r_1$. We obtain a parametric representation of system (6) for the periodic orbit as follows:

$$\varphi(\xi) = r_3 + (r_2 - r_3)\mathrm{sn}^2(\Omega_3\xi, k_7), \tag{48}$$

where, $k_7^2 = \frac{r_2 - r_3}{r_1 - r_3},\ \Omega_3 = \sqrt{2(r_1 - r_3)}$.

Thus, we obtain a periodic wave solution of equation (3) as follows:

$$u(x,t) = \left[r_3 + (r_2 - r_3)\mathrm{sn}^2(\Omega_3(x - ct), k_7)\right]^{\frac{1}{2}}. \tag{49}$$

(ii) Corresponding to the two stable manifolds and two unstable manifolds at $A_1(\phi_1, 0)$, that tends asymptotically to the singular straight line to $\phi = 0$ as $|y| \to \infty$, and an open curve passing through the point $P(r_1, 0)$, we have, the exact solutions of system (6) respectively:

$$\varphi(\xi) = r_2 + \frac{r_3 - r_2}{1 - \mathrm{sn}^2(\Omega_3\xi, k_7)}, \tag{50}$$

and

$$\varphi(\xi) = r_2 + \frac{r_1 - r_2}{1 - \mathrm{sn}^2(\Omega_3\xi, k_8)}, \tag{51}$$

where, $k_8^2 = \frac{r_1 - r_2}{r_1 - r_3}$.

Thus from equation (50) and (51) respectively, we obtain a compacton solution of equation (3) as follows:

$$u_{\{A_1\}}(x,t) = \left(r_2 + \frac{r_3 - r_2}{1 - \mathrm{sn}^2(\Omega_3(x - ct), k_7)} \right)^{\frac{1}{2}} \tag{52}$$

and

$$u_{\{P\}}(x,t) = \left(r_2 + \frac{r_1 - r_2}{1 - \mathrm{sn}^2(\Omega_3(x - ct), k_8)} \right)^{\frac{1}{2}}. \tag{53}$$

4.2. ***Parametric representation of exact wave solutions of equation (3) when*** $\alpha < 0$.**.** In this section, we give some exact explicit parametric representations of the traveling wave solutions such as solitary solutions, compacton solutions, periodic cusp wave solutions and periodic traveling wave solutions.

1. The case of $(\beta, \gamma) = (0, 0)$, $\Delta = h_0$**.** (see Fig. 5(a)).

In this case, $h_0 < h_1 < h_2$, $\varphi_l < 0 < \varphi_M$. For $h \ll 0$, the level curve defined by $H_3(\phi, y) = h$ (see Fig. 5(a)), there exists a homoclinic orbit to the cusp point $A_0(0, 0)$. Then from equation (41) we have

$$\int_{\varphi}^{\varphi_M} \frac{d\varphi}{\varphi\sqrt{(\varphi_M - \varphi)\varphi(\varphi - \varphi_l)}} = \left(2\sqrt{2}\right)\xi.$$

It follows the exact solutions of equation (6):

$$\varphi(\xi) = \varphi_M \mathrm{cn}^2(\Omega_4\xi, k_9), \tag{54}$$

where, $\Omega_4 = \sqrt{2(\varphi_M - \varphi_l)}$, $k_9^2 = \left(1 - \frac{\varphi_l}{\varphi_M}\right)^{-1}$.

Thus, we obtain a solitary wave solution of equation (3) as follows:

$$u(x, t) = \sqrt{\varphi_M}\mathrm{cn}(\Omega_4(x - ct), k_9). \tag{55}$$

Corresponding to the open arch curve to the left of the singular straight line $\phi = 0$, we have from equation (41) that:

$$\int_{\varphi_l}^{\varphi} \frac{d\varphi}{\varphi\sqrt{(\varphi_M - \varphi)\varphi(\varphi - \varphi_l)}} = \left(2\sqrt{2}\right)\xi.$$

It follows the exact solutions of equation (6):

$$\varphi(\xi) = \varphi_l \mathrm{cn}^2(\Omega_4\xi, k_{10}), \tag{56}$$

where, $k_{10}^2 = \left(1 - \frac{\varphi_M}{\varphi_l}\right)^{-1}$.

Thus, we obtain a compacton solution of equation (3) as follows:

$$u(x, t) = \frac{\sqrt{\varphi_l}}{\mathrm{nc}(\Omega_4(x - ct), k_{10})}. \tag{57}$$

2. The case of $(\beta, \gamma) \in C_2$, $h_2 = h_1 < h_0$**.** (see Fig. 5(e)). In this case, $r_3 < r_2 < r_1 < \varphi_M$ (i) For $h \ll 0$, the level curve defined by $H_3(\phi, y) = h$, there exists a family of homoclinic orbit to the equilibrium point $P(r_1, 0)$ enclosing the equilibrium point A_2. Then from equation (41) we have

$$\int_{\varphi}^{\varphi_M} \frac{d\varphi}{(\varphi - r_1)\sqrt{(\varphi_M - \varphi)(\varphi - r_2)(\varphi - r_3)}} = \left(2\sqrt{2}\right)\xi.$$

It follows the exact solutions of equation (6):

$$\varphi(\xi) = r_2 + \varphi_M \mathrm{cn}^2(\Omega_5\xi, k_{11}), \tag{58}$$

where, $\Omega_5 = \sqrt{2(\varphi_M - r_3)}$, $k_{11}^2 = \frac{\varphi_M - r_2}{\varphi_M - r_3}$.

Thus, we obtain a solitary wave solution of equation (3) as follows:

$$u(x,t) = \left(r_2 + \varphi_M \mathrm{cn}^2(\Omega_5(x-ct), k_{11})\right)^{\frac{1}{2}}. \tag{59}$$

(ii) Corresponding to the periodic orbit which encloses the equilibrium point $A_1(\phi_1, 0)$, we have from equation (41) that:

$$\int_{r_3}^{\varphi} \frac{d\varphi}{(r_1-\varphi)\sqrt{(\varphi_M-\varphi)(r_2-\varphi)(\varphi-r_3)}} = \left(2\sqrt{2}\right)\xi.$$

It follows the exact solutions of equation (6):

$$\varphi(\xi) = r_2 \mathrm{sn}^2(\Omega_5\xi, k_{12}) + r_3 \mathrm{cn}^2(\Omega_5\xi, k_{12}), \tag{60}$$

where, $k_{12}^2 = \frac{r_2 - r_3}{\varphi_M - r_3}$.

Thus, we obtain a periodic wave solution of equation (3) as follows:

$$u(x,t) = \left[r_2 \mathrm{sn}^2(\Omega_5(x-ct), k_{12}) + r_3 \mathrm{cn}^2(\Omega_5(x-ct), k_{12})\right]^{\frac{1}{2}}. \tag{61}$$

3. The case of $(\beta,\gamma) \in T_1^-$, $h_0 < h_2$**.** (see Fig. 5(f)).

For $h = h_0$, we have a family of periodic orbits of equation (6) shown in Fig. 5(f). We see from (7) that two arch curve connecting the equilibrium points $Q_1(0, -Y_s)$ and $Q_2(0, Y_s)$ in the left and right side of the straight line $\phi = 0$ enclosing the origin. Thus from (41) we have:

$$\int_{r_2}^{\varphi} \frac{d\varphi}{\sqrt{(r_1-\varphi)(\varphi-r_2)[(\varphi-\beta_1)^2+\beta_2^2]}} = \left(2\sqrt{2}\right)\xi.$$

It follows the exact solutions of equation (6):

$$\varphi(\xi) = \frac{r_1\mathrm{B}_1 + r_2\mathrm{A}_1 - (r_1\mathrm{B} - r_2\mathrm{A}_1)\mathrm{cn}(\Omega_6\xi, k_{13})}{\mathrm{A}_1 + \mathrm{B}_1 - (\mathrm{A}_1 - \mathrm{B}_1)\mathrm{cn}(\Omega_6\xi, k_{13})}, \tag{62}$$

where, $\Omega_6 = 2\sqrt{2\mathrm{A}_1\mathrm{B}_1}$, $k_{13}^2 = \frac{(r_1-r_2)^2-(A_1-B_1)^2}{4A_1B_1}$, $\mathrm{A}_1^2 = (r_1-\beta_1)^2+\beta_2^2$, $\mathrm{B}_1^2 = (r_2-\beta_1)^2+\beta_2^2$.

Thus, we obtain a periodic wave solution of equation (3) as follows:

$$u(x,t) = \left(\frac{r_1\mathrm{B}_1 + r_2\mathrm{A}_1 - (r_1\mathrm{B} - r_2\mathrm{A}_1)\mathrm{cn}(\Omega_6(x-ct), k_{13})}{\mathrm{A}_1 + \mathrm{B}_1 - (\mathrm{A}_1 - \mathrm{B}_1)\mathrm{cn}(\Omega_6(x-ct), k_{13})}\right)^{\frac{1}{2}}. \tag{63}$$

4. The case of $(\beta,\gamma) \in C_3$, $h_1 < h_0 < h_2$**.** (see Fig. 5(g)).

In this case we have $r_3 < 0 < r_2 < r_1$. For $h = h_1$, the level curve defined $H_3(\phi, y) = h$ there exists a family of periodic orbits and a homoclinic orbits.

(i) Corresponding to a homoclinic orbit at an equilibrium point $P(r_3, 0)$ enclosing the equilibrium point $A_1(\phi_1, 0)$. Thus from (41) we have:

$$\int_{\varphi}^{\varphi_M} \frac{d\varphi}{(\varphi - r_3)\sqrt{(\varphi_M - \varphi)(\varphi - r_2)(\varphi - r_1)}} = \left(2\sqrt{2}\right)\xi.$$

It follows the exact solutions of equation (6):

$$\varphi(\xi) = \varphi_M \mathrm{nc}^2(\Omega_7\xi, k_{14}) - r_2 \mathrm{tn}^2(\Omega_7\xi, k_{14}), \tag{64}$$

where, $\Omega_7 = \sqrt{(r_1 - \varphi_M)}$, $k_{14}^2 = \frac{r_1 - r_2}{r_1 - \varphi_M}$.

Thus, we obtain a solitary wave solution of equation (3) as follows:

$$u(x,t) = \left[\varphi_M \mathrm{nc}^2(\Omega_7(x - ct), k_{14}) - r_2 \mathrm{tn}^2(\Omega_7(x - ct), k_{14})\right]^{\frac{1}{2}}. \tag{65}$$

(ii) Corresponding to a family of periodic orbits of system (6), enclosing the equilibrium point $A_2(\phi_2, 0)$, we have from equation (41):

$$\int_{r_2}^{\varphi} \frac{d\varphi}{(\varphi - r_3)\sqrt{(\varphi - \varphi_M)(\varphi - r_2)(r_1 - \varphi)}} = \left(2\sqrt{2}\right)\xi.$$

It follows the exact solutions of equation (6):

$$\varphi(\xi) = \varphi_M + (r_2 - \varphi_M)\mathrm{nd}^2(\Omega_8\xi, k_{15}), \tag{66}$$

where, $\Omega_8 = \sqrt{2(r_1 - \varphi_m)}$, $k_{15}^2 = \frac{r_1 - r_2}{r_1 - \varphi_m}$.

Thus, we obtain a periodic wave solution of equation (3) as follows:

$$u(x,t) = \left[\varphi_M + (r_2 - \varphi_M)\mathrm{nd}^2(\Omega_8(x - ct), k_{15})\right]^{\frac{1}{2}}. \tag{67}$$

5. The case of $(\beta, \gamma) \in C_4$, $h_2 < h_0 < h_1$. (see Fig. 5(i)). In this case, $\varphi_m < r_3 < r_2 < r_1$.
(i) For $h \to 0$, the level curve defined by $H_3(\phi, y) = h$ (see Fig. 5(i)), there exists a homoclinic orbit to the equilibrium point $A_1(\phi_1, 0)$. Then from equation (41) we have

$$\int_{\varphi_m}^{\varphi} \frac{d\varphi}{(r_3 - \varphi)\sqrt{(\varphi - \varphi_m)(r_2 - \varphi)(r_1 - \varphi)}} = \left(2\sqrt{2}\right)\xi.$$

It follows the exact solutions of equation (6):

$$\varphi(\xi) = \varphi_m + (r_2 - r_1)\mathrm{sn}^2(\Omega_8\xi, k_{16}), \tag{68}$$

where, $k_{16}^2 = \frac{r_2 - \varphi_m}{r_1 - \varphi_m}$.

Thus, we obtain a solitary wave solution of equation (3) as follows (see Fig. 10(a)):

$$u(x,t) = \left[\varphi_m + (r_2 - r_1)\mathrm{sn}^2(\Omega_8(x - ct), k_{16})\right]^{\frac{1}{2}}. \tag{69}$$

(ii) Corresponding to a family of periodic orbits of system (6), enclosing the equilibrium point $A_2(\phi_2, 0)$. Then from equation (41) we have

$$\int_{r_2}^{\varphi} \frac{d\varphi}{(\varphi - r_3)\sqrt{(\varphi - \varphi_m)(\varphi - r_2)(r_1 - \varphi)}} = \left(2\sqrt{2}\right)\xi.$$

It follows the exact solutions of equation (6):

$$\varphi(\xi) = \varphi_m + (r_2 - \varphi_m)\mathrm{nd}^2(\Omega_8\xi, k_{16}), \tag{70}$$

Thus, we obtain a periodic wave solution of equation (3) as follows (see Fig. 10(b)):

$$u(x,t) = \left[\varphi_m + (r_2 - \varphi_m)\mathrm{nd}^2(\Omega_8\xi, k_{16})\right]^{\frac{1}{2}}. \tag{71}$$

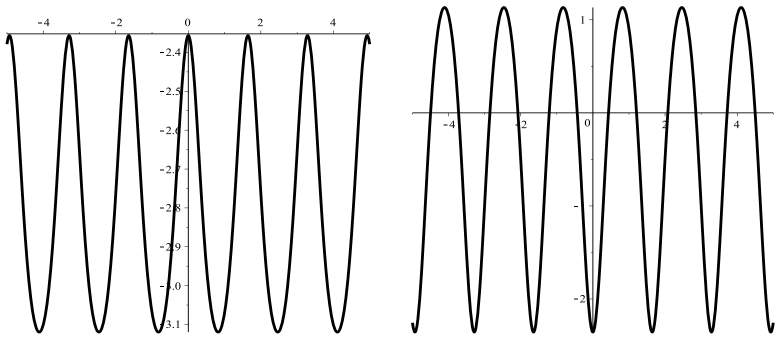

(a) Solitary wave. (b) Periodic wave.

FIGURE 10. Profile of solitary waves and periodic waves of system (6) when $(\beta, \gamma) \in C_4$ when $\alpha < 0$

Theorem 3: Depending on the changes of system parameters α, β, γ, the bifurcations of phase portraits of system (6) for $n = 3$ when $\alpha \in \mathbb{R}$ are shown in Fig. 1 (b), Fig. 4 and Fig. 5.

(i) Equation (3) has exact solitary wave solutions given by (43), (55), (65) and (69).

(ii) Equation (3) has exact compacton solutions given by (45), (52), (53) and (57).

(iii) Equation (3) has exact kink and anti-kink wave solutions given by (47).

(iv) Equation (3) has exact periodic wave solutions given by (49), (59), (61), (63), (67) and (71).

Theorem 4: Suppose that $n = 2m + 1$, $m \in \mathbb{Z}^+$ and see figure 4 and figure 5.

(1) For $(\beta, \gamma) = (0, 0)$, $\Delta = h_0$ When $\alpha \in \mathbb{R}$, equation (3) has a family of solitary wave solution at to the cusp point $A_0(0, 0)$ for $h \ll 0$.

(2) For $(\beta, \gamma) \in T_1^+$. When $\alpha > 0$, equation (3) has a couple of kink and anti-kink wave solutions for $h = h_1$ (or h_2), and has a family of uncountably infinite many periodic wave solutions for $h \in (h_1, +\infty)$. (3) For $(\beta, \gamma) \in C_1$. When $\alpha > 0$, equation (3) has two families of uncountably infinite many smooth periodic solutions for $h = h_0$, and has two stable manifolds and two unstable manifolds at $A_1(\phi_1, 0)$, that tends asymptotically to the singular straight line to $\phi = 0$ as $|y| \to \infty$.

(4) For $(\beta, \gamma) \in T_2^-$. When $\alpha < 0$, equation (3) has a family of uncountably infinite many smooth periodic solutions for $h = h_0$, and their amplitudes tend to $|y| \to \infty$ for $h \to 0$.
(5) For $(\beta, \gamma) \in C_4$. When $\alpha < 0$, equation (3) has two families of uncountably infinite many smooth periodic solutions enclosing the equilibrium point $A_2(\phi_2, 0)$ for $h \to 0$, and $|y| \to \infty$. And, also equation (3) has a family of smooth solitary wave solutions with peak (or valley) form for $h = h_0$

Acknowledgements

This research was partially supported by the National Natural Science Foundation of China (11471289, 11162020)

References

[1] M.J. Ablowitz, H. Segur, Solitons and the Inverse Scattering Transform, SIAM, Philadelphia, 1981.
[2] V.B. Matveev, M.A. Salle, Darboux Transformations and Solitons, Springer, Berlin, 1991.
[3] C.H. Gu, Soliton Theory and its Application, Springer, Berlin, 1995.
[4] E.G. Fan, Extended tanh-function method and its applications to nonlinear equations, Phys. Lett. A, **277** (2000) 212-218.
[5] Y. Kivshar, Compactons in discrete lattices, Nonlinear Coherent Struct. Phys. Biol. **329** (1994) 255-258.
[6] P.T. Dinda, M. Remoissenet, Breather compactons in nonlinear Klein-CGordon systems, Phys. Rev. E **60 (3)** (1999) 6218-6221.
[7] P. Rosenau, J.M. Hyman, Compactons: solitons with finite wavelengths, Phys. Rev. Lett. **70 (5)** (1993) 564-567.
[8] A.M. Wazwaz, Partial Differential Equations: Methods and Applications, Balkema Publishers, The Netherlands, 2002.
[9] A.M. Wazwaz, Compactons and solitary patterns structures for variants of the KdV and the KP equations, Appl. Math. Comput. **139 (1)** (2003) 37-54.
[10] A.M. Wazwaz, Explict travelling wave solutions of variants of the K(n,n) and ZK(n,n) equations with compact and noncompact structures, Appl. Math. Comput., **173** (2006) 213-230.
[11] J. B. Li, Singular nonlinear traveling wave equations: bifurcation and exact solutions, Science, Beijing, 2013.
[12] J. B. Li, G. R. Chen, On a class of singular nonlinear traveling wave equations, Int. J. Bifurcation Chaos, **17** (2007) 4049-4065.
[13] A. A. Andronov, E. A. Leontovich, J. I. Gordon; Theory of bifurcations of dynamical systems on a plane, Wiley, New York, 1973.
[14] J. Guckenheimer and P. J. Holmes, Nonlinear Oscillations, Dynamical Systems and Bifurcations of Vector Fields, Springer-Verlag, NewYork, 1983.
[15] L. Temesgen Desta, J. B. Li, Dynamical behavior and exact solution in invariant manifold for a thirteenth derivative nonlinear Schrödinger equation, J. Appl. Anal. Comput. **8(1)** 2018 250-271(21 pages)
[16] P. F. Byrd, M. D. Fridman, Handbook of elliptic intrgrals for engineers and sciensists, Springer, Berlin, 1971.